

# Thin Absolute Villains

*C.F. Baillie*

Computer Science Dept.  
University of Colorado  
Boulder, CO 80309, USA

*N. Dorey*

Department of Physics  
Universite of Wales Swansea  
Swansea, SA2 8PP, Wales

*W. Janke*

Institut für Physik  
Johannes Gutenberg-Universität  
D-55099 Mainz, Germany

and

*D.A. Johnston*

Dept. of Mathematics  
Heriot-Watt University  
Edinburgh, EH14 4AS, Scotland

November 15, 2018

## Abstract

We perform simulations of an absolute value version of the Villain model on  $\phi^3$  and  $\phi^4$  Feynman diagrams, “thin” 3-regular and 4-regular random graphs. The  $\phi^4$  results are in excellent quantitative agreement with the exact calculations by Dorey and Kurzepa for an annealed ensemble of thin graphs, in spite of simulating only a *single* graph of each size. We also derive exact results for an annealed ensemble of  $\phi^3$  graphs and again find excellent agreement with the numerical data for single  $\phi^3$  graphs.

The simulations confirm the picture of a mean field vortex transition which is suggested by the analytical results. Further simulations on  $\phi^5$  and  $\phi^6$  graphs and of the standard XY model on  $\phi^3$  graphs confirm the universality of these results. The calculations of Dorey and Kurzepa were based on reinterpreting the large orders behaviour of the anharmonic oscillator in a statistical mechanical context so we also discuss briefly the interpretation of singularities in the large orders behaviour in other models as phase transitions.

# 1 Background and Calculations

It has long been known that mean field behaviour is found in models with short range interactions living on tree-like structures such as Bethe lattices [1]. This approach circumvents some of the problems that appear with using infinite range interactions to get mean field results. Difficulties still arise, however, both analytically and numerically when dealing with the dominant boundary of such trees. Random graphs, which are locally tree-like and have no external legs, offer a way round this problem, giving a way of calculating and simulating models on closed lattices with short range interactions that still behave in a mean field like manner.

There has been a considerable amount of work on spin glass models on random graphs [2] mostly with Ising or Potts spins, often based on analogy with the corresponding Bethe lattice. Recently it was pointed out that transplanting methods from matrix models and 2D quantum gravity allowed a considerable simplification of many of the proofs that had been derived [3] and offered the possibility of attacking problems like replica symmetry breaking from a different perspective. In effect one considers a  $d = 0$ ,  $N = 1$  matrix, or scalar, model where  $N$  is the size of the matrix, to generate the requisite ensemble of random graphs in a Feynman diagram expansion. For large enough graphs saddle point methods can be employed and the mean field critical behaviour calculated from the algebraic saddle point equations<sup>1</sup>.

The matrix model inspired approach to discrete spin models was predated by independent work on the finite temperature quantum mechanics of the anharmonic oscillator, interpreted as a  $d = 1$ ,  $N = 1$  matrix model [5]. This described a Villain transcription of the continuous spin  $XY$  model on  $\phi^4$  graphs and gave a mean field vortex transition rather than the Kosterlitz-Thouless ( $KT$ ) [6] transition of the standard two dimensional  $XY$  model. In essence, the thermodynamic limit of the  $\phi^4$  random graph model is described by large orders in the perturbation series of the anharmonic oscillator in finite temperature quantum mechanics.

Part of the original motivation for considering the  $XY$  model transition on an ensemble of random graphs was the study of the  $XY$  model coupled to 2D quantum gravity. This is equivalent to putting the discretized model on an annealed ensemble of *fat*, or planar, graphs. Calculations [7] and simulations [8] have both indicated that the transition was still  $KT$  in nature in such an ensemble, but a definitive proof of this has been elusive. The idea in [5] was to find an ensemble of graphs in which complete calculations *were* possible and in which some sort of transition was still manifest. An ensemble of generic “thin” random graphs proved to be such a case.

If we write the finite temperature partition function for the anharmonic oscillator as

$$Z(\beta, g) = \int D\phi \exp \left( - \int_0^\beta d\tau \left[ \frac{1}{2} \dot{\phi}^2 + \frac{1}{2} \phi^2 + g\phi^4 \right] \right), \quad (1)$$

where  $\beta = 1/T$  is the inverse temperature, and carry out the perturbative expansion in  $g$ ,

$$Z(\beta, g) \simeq \sum_{k=0}^{\infty} Z_k(\beta) g^k, \quad (2)$$

then each  $Z_k(\beta)$  may be written as a sum over Feynman diagrams, which in this case are random  $\phi^4$  graphs with  $k$  vertices, giving

$$Z_k(\beta) = (-1)^k \sum_G S(G) \int_0^\beta \dots \int_0^\beta \prod_{i=1}^k dt_i \prod_{\langle ij \rangle} \sum_{m_{ij}=-\infty}^{\infty} \exp(-|t_i - t_j + m_{ij}\beta|). \quad (3)$$

In the above  $S(G)$  is the symmetry factor, which will generically be unity for a large graph, the  $t_i$  are attached to each vertex and integrated over 0 to  $\beta$ , and the  $m_{ij}$  are attached to each link and summed over the integers. The partition function  $Z_k(\beta)$  can be thought of as coming from embedding the  $\phi^4$  graph on a circle of period  $\beta$ . The finite temperature one-dimensional propagator that appears in the above,

$$D_{\langle ij \rangle} = \sum_{m_{ij}=-\infty}^{\infty} \exp(-|t_i - t_j + m_{ij}\beta|), \quad (4)$$

---

<sup>1</sup>Inverting the logic of such an approach to use statistical mechanical methods to investigate the large orders behaviour of Feynman diagram expansions was actually suggested some years ago by Bender and Wu [4].

assigns a time coordinate  $t_{i,j}$  to each end of an edge as well as a winding number  $m_{ij}$  to the edge itself. Written in this form the similarity with the Villain version of the XY model [9], where the edge factor is

$$\tilde{D}_{\langle ij \rangle} = \sum_{m_{ij}=-\infty}^{\infty} \exp\left(-\frac{\beta}{2}(\theta_i - \theta_j + 2\pi m_{ij})^2\right), \quad (5)$$

with  $\theta$  taking values in the interval 0 to  $2\pi$ , is apparent so we might expect the same sort of critical behaviour. We have, in effect, interpreted the finite temperature quantum mechanics of the anharmonic oscillator as an absolute value version of the Villain model living on thin random graphs.

For convenience here we perform a rescaling of the  $t_i$  to obtain

$$Z_k(\beta) = (-1)^k \beta^k \sum_G S(G) \int_0^1 \dots \int_0^1 \prod_{i=1}^k dt_i \prod_{\langle ij \rangle} \sum_{m_{ij}=-\infty}^{\infty} \exp(-\beta|t_i - t_j + m_{ij}|), \quad (6)$$

which will simplify some of the later formulae for quantities to be measured in the simulations. As in [5] the free energy per vertex is defined as

$$F = - \lim_{k \rightarrow \infty} \frac{1}{k} \log | \frac{Z_k(\beta)}{n_k} |, \quad (7)$$

where  $n_k$  is the number of graphs of size  $k$ ,  $n_k \simeq (16)^k (k-1)!$ . Note that, in this case, the thermodynamic limit is taken by setting  $k \rightarrow \infty$  by hand. Unlike the case of planar diagrams and two dimensional gravity there is no cosmological constant dual to the area that one can tune to induce critical behaviour.

The energy per vertex in the model  $\rho = \partial F / \partial \beta$  measures the expectation value of the target-space length of the embedded graph, as can be seen by differentiating the Laplace transform of  $Z_k(\beta)$ ,

$$Z_k(\beta) = \int_0^{\infty} dL \tilde{Z}_k(L) \exp(-L\beta), \quad (8)$$

with respect to  $\beta$ . As discussed in [5],  $\rho$  can be interpreted as a measure of the density of vortices in the model. The specific heat is also given by the standard formula

$$C = -\beta^2 \frac{\partial^2 F}{\partial \beta^2}, \quad (9)$$

or equivalently by directly differentiating the energy  $C = \partial \rho / \partial T$ .

The analytical solution of the thin graph model proceeds by looking at the large orders behaviour of the anharmonic oscillator partition function [10] in equ.(1). After a rescaling  $x = 2\sqrt{-g}\phi$ , the  $k \rightarrow \infty$  saddle point solution is given by the trajectories of period  $\beta$  of a particle moving in the potential  $V = -\frac{1}{2}x^2 + \frac{1}{4}x^4$ . One uses the dispersion relation,

$$Z_k(\beta) = \frac{1}{\pi} \int_{-\infty}^0 dg \frac{\text{Im}Z(\beta, g + i0)}{g^{k+1}}, \quad (10)$$

along with the saddle-point evaluation of  $\text{Im}Z(\beta, g)$  to extract  $Z_k(\beta)$ . A non-trivial instanton solution only exists above a critical value of the period  $\beta$  (in the  $\phi^4$  case  $\beta_c = \sqrt{2}\pi$ ). For  $\beta < \beta_c$  the only contribution is from the trivial solution  $x(t) \equiv x_{\min}$ , where the particle sits at the bottom of the well. The change of behaviour at  $\beta = \beta_c$  is taken as the signal for a phase transition in the associated absolute value Villain model. In the low temperature phase we find

$$Z_k \simeq (-1)^k \frac{\beta}{2} \left( \frac{1}{2\pi} \frac{\partial E}{\partial \beta} \right)^{1/2} [I(\beta)/4]^{-(k+1/2)} \Gamma(k + 1/2), \quad (11)$$

while for  $\beta < \beta_c$ ,

$$Z_k \simeq (-1)^k 2 \left( \frac{\sqrt{2} \sinh(\beta)}{\sinh(\sqrt{2}\beta)} \right)^{1/2} \left( \frac{\beta}{16} \right)^{-k} \Gamma(k). \quad (12)$$

In the above  $I(\beta)$  is just the (scaled) classical action of the instanton satisfying

$$\frac{\partial I(\beta)}{\partial \beta} = -E(\beta), \quad (13)$$

where  $E(\beta)$  is the energy associated with this trajectory. To obtain explicit expressions in the above we need to determine the dependence of  $E$  on the period  $\beta$ . This can be done by evaluating the first integral of the classical equations of motion,

$$\beta(E) = 2 \int_{x_1}^{x_2} \frac{dx}{\sqrt{2[E - V(x)]}}, \quad (14)$$

where  $x_1$  and  $x_2$  are the turning points. In the  $\phi^4$  case, the above integral can be evaluated perturbatively near  $\beta_c$  [5]. Inverting the power series gives  $E(\beta) = -1/4 + 4(\beta - \beta_c)/(3\beta_c) + \dots$ . These solutions predict  $\rho = 1/\beta$  for  $\beta < \beta_c$  and  $\rho \simeq \exp(-\beta)$  at large  $\beta$ . Similarly  $C = 1$  for  $\beta < \beta_c$  and sweeps up to a sharp cusp of height  $19/3$  as  $\beta \rightarrow \beta_c+$ . In order to obtain the full temperature dependence of  $\rho$  and  $C$  shown in Figs. 1 and 2, we found it useful to express both  $\beta(E)$  and the (scaled) classical action in terms of elliptic integrals, which can easily be evaluated with high precision. In summary, we see a second order transition of the mean-field type, with a sharp cusp discontinuity in the specific heat.

An explicit calculation can also be carried through in a similar style for the  $\phi^3$  case where the partition function is

$$Z(\beta, g) = \int D\phi \exp \left( - \int_0^\beta d\tau \left[ \frac{1}{2} \dot{\phi}^2 + \frac{1}{2} \phi^2 + g\phi^3 \right] \right). \quad (15)$$

After a rescaling  $x = -3g\phi$ , the problem is mapped onto considering the trajectories of a particle in the potential  $= -\frac{1}{2}x^2 + \frac{1}{3}x^3$ . The relation (13) between the classical action and the energy can be solved, as in the  $\phi^4$  case, by inverting the relation for  $\beta(E)$  to get  $E(\beta)$ . Here we find

$$\beta = 6^{1/3} \frac{2K(k)}{\sqrt{x_3 - x_1}}, \quad (16)$$

where  $K$  is the complete elliptic integral with modulus  $k = \sqrt{(x_3 - x_2)/(x_3 - x_1)}$ , and  $x_1 < x_2 < x_3$  are the roots of  $2[E - V(x)] = 2E + x^2 - 2x^3/3 = 0$ . Inverting gives  $E(\beta) = -1/6 + 6(\beta - \beta_c)/(5\beta_c) + \dots$ , where  $\beta_c$  is now  $2\pi$ . The form of  $\rho$  and  $C$  is similar to the  $\phi^4$  graphs, but we now find a peak of  $41/10$  in  $C$  as  $\beta \rightarrow \beta_c+$  and  $C = 1/2$  for  $\beta < \beta_c$ . As in the  $\phi^4$  case, to compute the full temperature dependence of  $\rho$  and  $C$ , we first expressed the (scaled) classical action in terms of elliptic integrals,

$$I = \frac{4}{15} \sqrt{\frac{2}{3}} (x_3 - x_1)^{5/2} \left[ (2 - 2k^2 + 2k^4)E(k) - (2 - 3k^2 + k^4)K(k) \right] - E\beta. \quad (17)$$

A couple of other numerical consequences of the analytical results are worth remarking upon as they are convenient for verifying that simulations are performing correctly. Firstly, we find that  $\rho(T_c)$  is equal to  $T_c$  on  $\phi^4$  graphs. Secondly, it should be noted that the  $\beta_c$  is determined only by the period of oscillations around the minimum of the potential for *any* potential. Approximating this region with a quadratic gives  $\beta_c = 2\pi/m$  if  $V \simeq -V_0 + m^2(x - x_0)^2/2$ , where  $x_0$  is the minimum point. This reproduces the explicit results derived above for  $\phi^3$  and  $\phi^4$  graphs with rather less pain. Finally, it is worth noting that, for a potential with an anharmonic term of the form  $\phi^{2(p+1)}$ , we will have  $C = p$  for  $T \geq T_c$  because  $\rho = pT$  for  $T \geq T_c$  in general.

We can contrast the critical behaviour described above with the standard  $XY$  model on a flat two dimensional lattice

$$Z = \prod_i \left[ \int_0^{2\pi} d\theta_i \right] \exp \left( \beta \sum_{\langle ij \rangle} \cos(\theta_i - \theta_j) \right), \quad (18)$$

which displays a topologically driven Kosterlitz-Thouless (KT) transition. The specific heat has only a broad cusp rather than a divergence. However, the correlation length has a critical singularity

$$\xi = A_\xi \exp \left( \frac{B_\xi}{(T - T_c)^\nu} \right), \quad (19)$$

as does the spin susceptibility

$$\chi = A_\chi \exp\left(\frac{B_\chi}{(T - T_c)^\nu}\right). \quad (20)$$

The exponent  $\nu$  is predicted to be 1/2 in the KT theory and the correlation function critical exponent is predicted to be  $\eta = 1/4$ , where  $\eta$  is given by

$$\chi \propto \xi^{2-\eta}. \quad (21)$$

In spite of the differences the physical picture of the transition on thin graphs is still very similar to that of the standard KT transition. Given the interpretation of  $\rho$  as a vortex density, the preceding saddle point results show that as the temperature is increased (ie  $\beta$  is decreased) vortices are liberated, with the vortex density increasing by almost an order of magnitude around  $\beta_c$ .

As we have already noted, it is not a foregone conclusion that putting the model on *any* collection of random graphs will give mean field behaviour - the model still displays a KT transition on an annealed set of planar random graphs (ie when coupled to 2D quantum gravity). An explicit check of the thin graph predictions is therefore not totally vacuous. In what follows we describe some modest simulations that we carried out in order to verify the mean field nature of the transition for variants of the model on various thin graphs. We are essentially interested in the behaviour of the energy and specific heat with  $\beta$  and determining  $\beta_c$ . We simulated the absolute value Villain action on  $\phi^3, \phi^4, \phi^5$  and  $\phi^6$  random graphs, as well as looking at the standard  $XY$  action of equ.(18) on  $\phi^3$  graphs in order to check it had the same critical behaviour.

## 2 Simulations

We need to exercise a little care in defining our observables in the simulation because of the unusual form of the Boltzmann factors in the partition function [11]. If we define the auxiliary sums

$$\begin{aligned} \Sigma_0 &= \sum_{m_{ij}=-\infty}^{\infty} \exp(-\beta|t_i - t_j + m_{ij}|), \\ \Sigma_1 &= \sum_{m_{ij}=-\infty}^{\infty} |t_i - t_j + m_{ij}| \exp(-\beta|t_i - t_j + m_{ij}|), \\ \Sigma_2 &= \sum_{m_{ij}=-\infty}^{\infty} |t_i - t_j + m_{ij}|^2 \exp(-\beta|t_i - t_j + m_{ij}|), \end{aligned} \quad (22)$$

then the definition of the energy  $\rho = \partial F / \partial \beta$  applied to the partition function in equ.(6) gives

$$\rho = \frac{1}{k} \left\langle \sum_{\langle ij \rangle} \frac{\Sigma_1}{\Sigma_0} \right\rangle - \frac{1}{\beta} \quad (23)$$

for the energy per site, where the  $\langle \rangle$  denote a thermal average and the additional  $1/\beta$  comes from the overall factor of  $\beta^k$  that appears when the  $t_i$  are rescaled.

The specific heat can be obtained in the simulations either by direct numerical differentiation of the measurements of  $\rho$  using  $C = \partial \rho / \partial T$ , or by differentiating equ.(6) twice to give

$$C = \beta^2 k (\langle \rho^2 \rangle - \langle \rho \rangle^2) + \frac{\beta^2}{k} \left\langle \sum_{\langle ij \rangle} \left( \frac{\Sigma_2}{\Sigma_0} - \frac{\Sigma_1^2}{\Sigma_0^2} \right) \right\rangle - 1. \quad (24)$$

The second term is non-canonical and is due to the summed Boltzmann factors whereas the  $-1$  results from the overall  $\beta^k$ .

Having decided on our observables, it now remains to choose an update scheme for the simulation. A simple Metropolis update can be used quite efficiently by adopting a discrete approximation to the periodic  $t_i$  and then tabling the resulting Boltzmann factors and associated sums  $\Sigma_{0,1,2}$ , which can then be looked up during the course of the simulation [11]. Depending on the temperature, we took from 100

to 1000 different  $t$  values for the tables, which were constructed by truncating the sum over  $m_{ij}$  at  $\pm 100$ . Increasing these limits made no appreciable difference to the measured results in any of the simulations reported here. In doing this we are taking a  $Z_{100} \dots Z_{1000}$  approximation to the  $O(2)$  symmetry of the model. Notice that for the absolute value version of the Villain model one has to be quite careful with this approximation, in particular at low temperatures, since the associated discretization error enters linearly in the action and not squared as in the standard Villain model. It is perhaps worth remarking that one could equally well envisage leaving the  $m_{ij}$  as free variables on each link to be sampled in the course of the simulation, but previous work in which the sum is carried out *a priori* as here has given good results for the standard Villain/XY model [11] and we stick to this. The direct form of  $D_{\langle ij \rangle}$  converges rapidly for large  $\beta$ , but is also possible to use a “dual” representation that is best suited for small  $\beta$  simulations,

$$\tilde{D}_{\langle ij \rangle} = \frac{2}{\beta} \left( 1 + \sum_{k_{ij}=1}^{\infty} \frac{\cos(2\pi k_{ij}(t_i - t_j))}{1 + \left(\frac{2\pi k_{ij}}{\beta}\right)^2} \right). \quad (25)$$

The numerical differences, even when using the representations well into the “wrong” regions of  $\beta$  for both, are slight.

The final ingredient in the simulations is the choice of a random graph. The calculations we have outlined in the first section are supposedly for an annealed ensemble of thin graphs, so in theory we should carry out “flip” moves in the same fashion as in simulations of 2D gravity on planar graphs. However, we can evade this responsibility by appealing to previous simulations of the Ising model on random graphs [3], where a *single* random graph of a given size was enough to extract the mean field critical behaviour predicted in an annealed calculation. As the thin random graphs are essentially tree-like it appears that one tree is very much like another as far as a ferromagnetic transition is concerned, although a (quenched) average over graphs becomes essential when non-self-averaging transitions such as those in spin glasses are simulated. We shall take the lazy man’s approach here and verify that the single graph results are consistent with the analytical calculations that, strictly speaking, only apply to an annealed ensemble.

We simulated the absolute value Villain model of equ.(6) on  $\phi^3$  and  $\phi^4$  graphs of size up to 2500 vertices, as well as small runs of  $N = 250$   $\phi^5$  and  $\phi^6$  graphs. In all the cases we carried out 500,000 Metropolis sweeps at each  $\beta$  value, with a measurement every tenth sweep, after allowing a suitable amount of equilibration time. As we have indicated *no* flip moves were carried out on the graphs concerned. The energy and specific heat, defined as above, were the principal observables. In addition, we also simulated the standard XY model of equ.(18) on  $\phi^3$  graphs, using a single cluster update, largely as a check on the universality of the Villain model results.

Turning now to the results themselves we can see in Fig. 1 that the energy matches closely the predictions of [5]. There is a low temperature exponential growth with a “knee” at the phase transition  $T = 1/\sqrt{2\pi} (\simeq 0.225)$  followed by linear growth at larger  $T$ . It is also clear from Fig. 1 that  $\rho(T_c) = T_c$ , as predicted by the analysis in the previous section. We can obtain the specific heat either from direct differentiation of the energy or by measuring the observable defined in equ.(24), and both are plotted in Fig. 2 for a graph of size 1000. This is the smallest graph size at which the peak reaches its expected value (19/3) - larger graphs give similar results, whereas the peak is appreciable lower and more rounded on the smaller graphs simulated. Surprisingly, it is the numerical differentiation that gives the closest fit to the analytical results, perhaps an indication that our statistics around the phase transition point are rather too modest for complete numerical accuracy in quantities involving variances, such as the directly measured specific heat.

Fortified by the good agreement between the analytical and numerical results for  $\phi^4$  graphs we can move on to look at the possible variations on the theme that were outlined in the introduction. We consider the  $\phi^3$  graphs first. In Fig. 3 we plot the energy for various graph sizes, showing clearly the similarity with the  $\phi^4$  results. The “knee” in the curve is at the expected value of  $T_c = 1/2\pi \simeq 0.16^2$ . As our data points are rather scarcer than for the  $\phi^4$  graphs, the specific heat peak obtained by numerical differentiation as shown in Fig. 4 is not so convincing, but it is clearly of the same general form and has the correct large  $T$  limit of  $1/2$ .

We have not carried out such extensive simulations of the  $\phi^5$  and  $\phi^6$  random graphs, simply contenting ourselves with verifying that the general form of the energy is similar and that the large  $T$  limit is correct.

<sup>2</sup>In this case, however, we do not expect that  $\rho(T_c) = T_c$ , but rather  $\rho(T_c) = T_c/2$ .

In Fig. 5 the energy is plotted up to very large  $T$  for  $\phi^3, \phi^4, \phi^5$  and  $\phi^6$  graphs of size 250. From the slopes it is clear that the specific heat prediction  $C \rightarrow p$  for  $T \rightarrow \infty$  on  $\phi^{2(p+1)}$  graphs is satisfied to a high degree of accuracy. The finite size effects for a given graph size increase with the degree of the vertices, which agrees with the intuitive picture of  $\phi^{2(p+1)}$  graphs being more “tree-like” for smaller  $p$  with a given number of vertices.

All of the simulations and discussions so far have dealt with the absolute value Villain model on various random graphs. We have done this because the edge factor in this case is just the one dimensional finite temperature propagator of equ.(4), which allows us to borrow (steal!) the results from large orders expansion of various anharmonic oscillators. We would expect that the standard XY model of equ.(14) would still give us similar results on grounds of universality, but as we have no analytical calculations to fall back on in this case it is worthwhile verifying this explicitly with simulations. We therefore simulated the standard XY model on  $\phi^3$  graphs of various sizes, with similar statistics to the Villain model simulations but using a single cluster update for improved efficiency.

The specific heat, measured directly in the simulation, is plotted in Fig. 6 for various lattice sizes, where it is clear that, although the small and large  $T$  limits are different from the Villain models (1/2 and 0 respectively), there is still a sharp cusp in the curve. This would again indicate a transition of mean field rather than  $KT$  type, where there is a much gentler bump in the specific heat curve away from the phase transition point.

As for the standard Villain model [12], the differences can be understood by an approximate mapping of the absolute value version of the Villain model onto the cosine model. By adapting the formulas in [12] to the present case, we find that the temperature scales should be related by  $I_1(\beta^{\text{cos}})/I_0(\beta^{\text{cos}}) = (\beta/2\pi)^2 / (1 + (\beta/2\pi)^2)$ , where  $I_{0,1}$  are Bessel functions and  $\beta^{\text{cos}}$  denotes the inverse temperature of the cosine model. Inserting  $\beta_c = 2\pi$  this predicts  $I_1(\beta_c^{\text{cos}})/I_0(\beta_c^{\text{cos}}) = 1/2$  or  $T_c^{\text{cos}} = 0.8625\dots$ , in good agreement with the peak location observed in Fig. 6.

### 3 Conclusions and Other Models

The saddle point predictions for the energy and specific heat of the absolute value Villain model on various random graphs are verified by the simulations we have carried out. As one might expect the standard XY model on “thin”  $\phi^3$  graphs behaves in an analogous fashion, with a mean-field-like transition rather than a  $KT$  transition. The second point worth emphasizing is that we have not needed to simulate an annealed ensemble of random graphs to get good *quantitative* agreement with the theory, just as for the Ising ferromagnet on thin graphs [3]. This should be contrasted with the planar graphs in 2D gravity where an annealed sum, usually implemented by flip moves in a simulation, appears to be essential. It appears that, unless one is very unlucky, any large thin graph is as good as another. Trees, and the near trees that thin random graphs represent, all really do look much alike.

The methods used in deriving the analytical results are borrowings from standard large orders lore in quantum mechanics. It is rather the interpretation in terms of a statistical mechanical model that is novel, just as the behaviour of discrete spin models on random graphs is extracted from known saddle points results for ordinary integrals in [3]. We are not restricted to the simple anharmonic oscillator in searching for statistical mechanical interpretations of large orders behaviour in quantum mechanics. Another possible example was considered by one of the authors of this paper in [13], namely the quantum mechanics of an anisotropic anharmonic oscillator, where the partition function is

$$Z = \int D\phi_1 D\phi_2 \exp \left( - \int_0^\beta d\tau \left[ \frac{1}{2}(\dot{\phi}_1^2 + \dot{\phi}_2^2 + \phi_1^2 + \phi_2^2) + g(\phi_1^4 + 2c\phi_1^2\phi_2^2 + \phi_2^4) \right] \right). \quad (26)$$

Taking  $c$  as the control parameter rather than  $\beta$ , the large orders behaviour shows a transition at  $c = 1$ , where the model is rotationally symmetric. For  $-1 \leq c < 1$  the quartic  $\phi_1^4 + \phi_2^4$  terms dominate and the instanton solution is  $\phi_1(t) = u(t), \phi_2(t) = 0$ , where

$$u(t) = \sqrt{\frac{1}{2|\lambda|} \frac{1}{\cosh(t - t_0)}}, \quad (27)$$

whereas for  $c > 1$  the  $\phi_1^2\phi_2^2$  term dominates and the solution is of the form  $\phi_1(t) = \phi_2(t) = u(t)/\sqrt{2}$ . Looking at the Feynman diagrams generated by the model we can see that it is a sort of loop gas, with  $\phi_1$

loops and  $\phi_2$  loops mixing via the  $\phi_1^2\phi_2^2$  vertex and a propagator  $D_{\langle ij \rangle}$  between the individual vertices on loops of both types. A matrix model style order parameter can be defined as

$$M = \frac{\phi_1^4 - \phi_2^4}{\phi_1^4 + \phi_2^4}, \quad (28)$$

which, using the instanton solutions, gives  $M = 1$  for  $-1 \leq c < 1$  and  $M = 0$  for  $c > 1$ . Alternatively, we could consider the ratio of mixed to pure vertices,

$$\tilde{M} = 1 - \frac{2\phi_1^2\phi_2^2}{\phi_1^4 + \phi_2^4}, \quad (29)$$

with similar results. With either order parameter we can see that the random graphs are filled with  $x$  loops only for  $-1 \leq c < 1$  and an even mixture of  $x$  and  $y$  loops for  $c > 1$ . The singular behaviour at  $c = 1$  can thus be viewed as a sort of magnetization transition.

It would be an interesting exercise to see if other large orders results in quantum mechanics could be recast in a statistical mechanical mould as in this case. We leave this for future work.

## 4 Acknowledgements

CFB is supported by DOE under contract DE-FG02-91ER40672 and by NSF Grand Challenge Applications Group Grant ASC-9217394. ND is supported by a PPARC advanced fellowship. WJ thanks the Deutsche Forschungsgemeinschaft for a Heisenberg fellowship. This work has been carried out in the framework of the EC HCM network grant ERB-CHRX-CT930343.

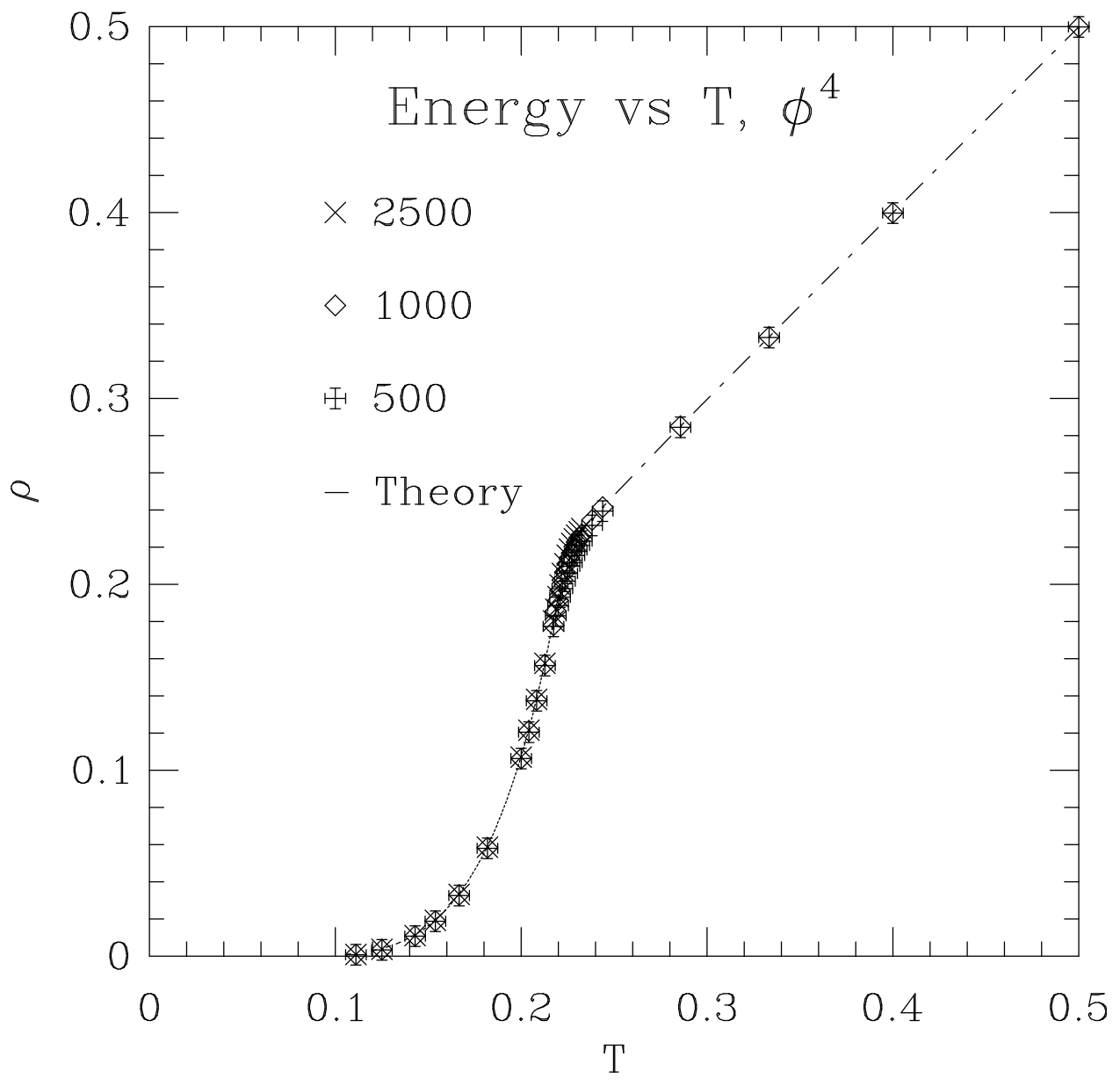


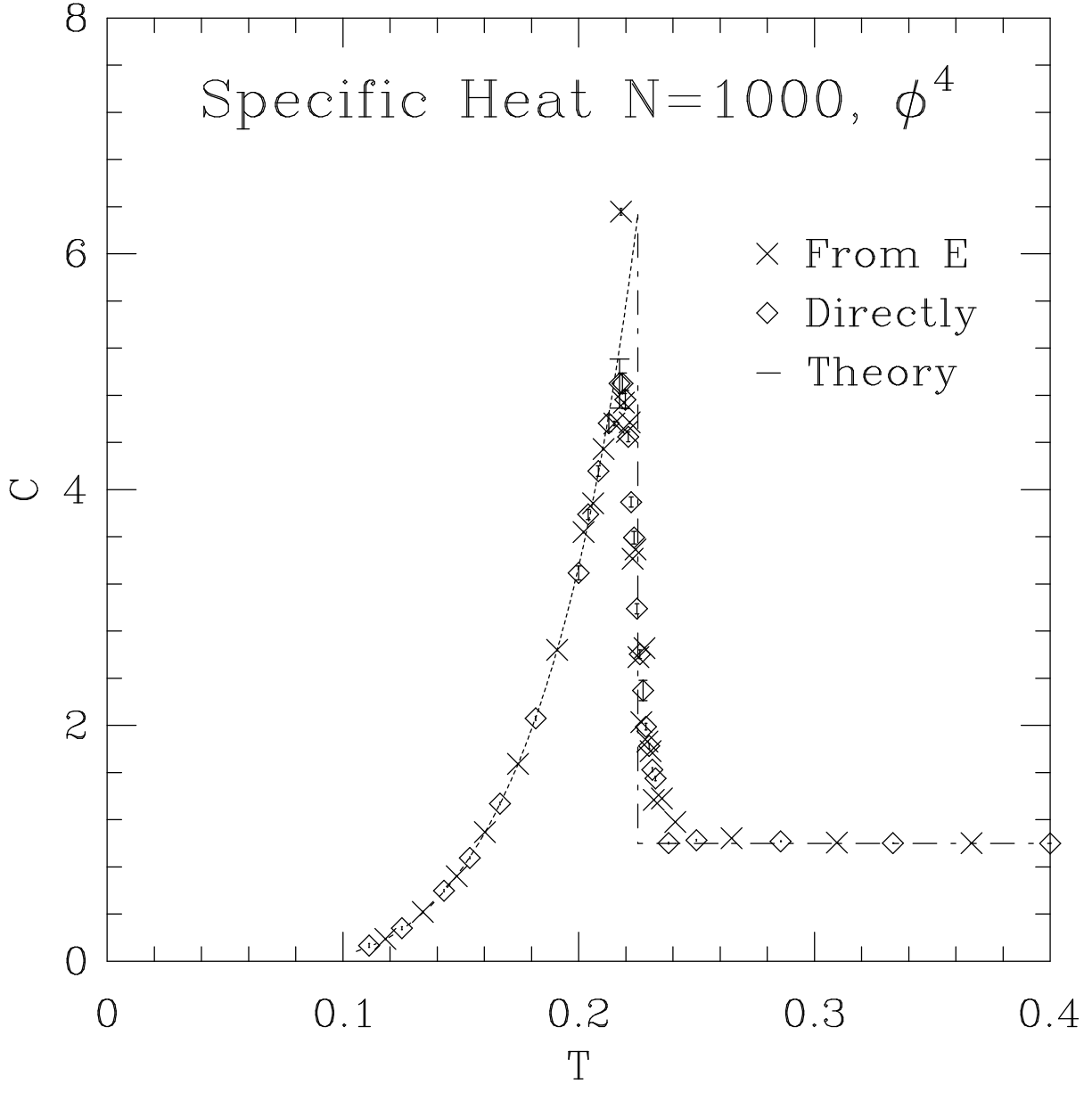
## References

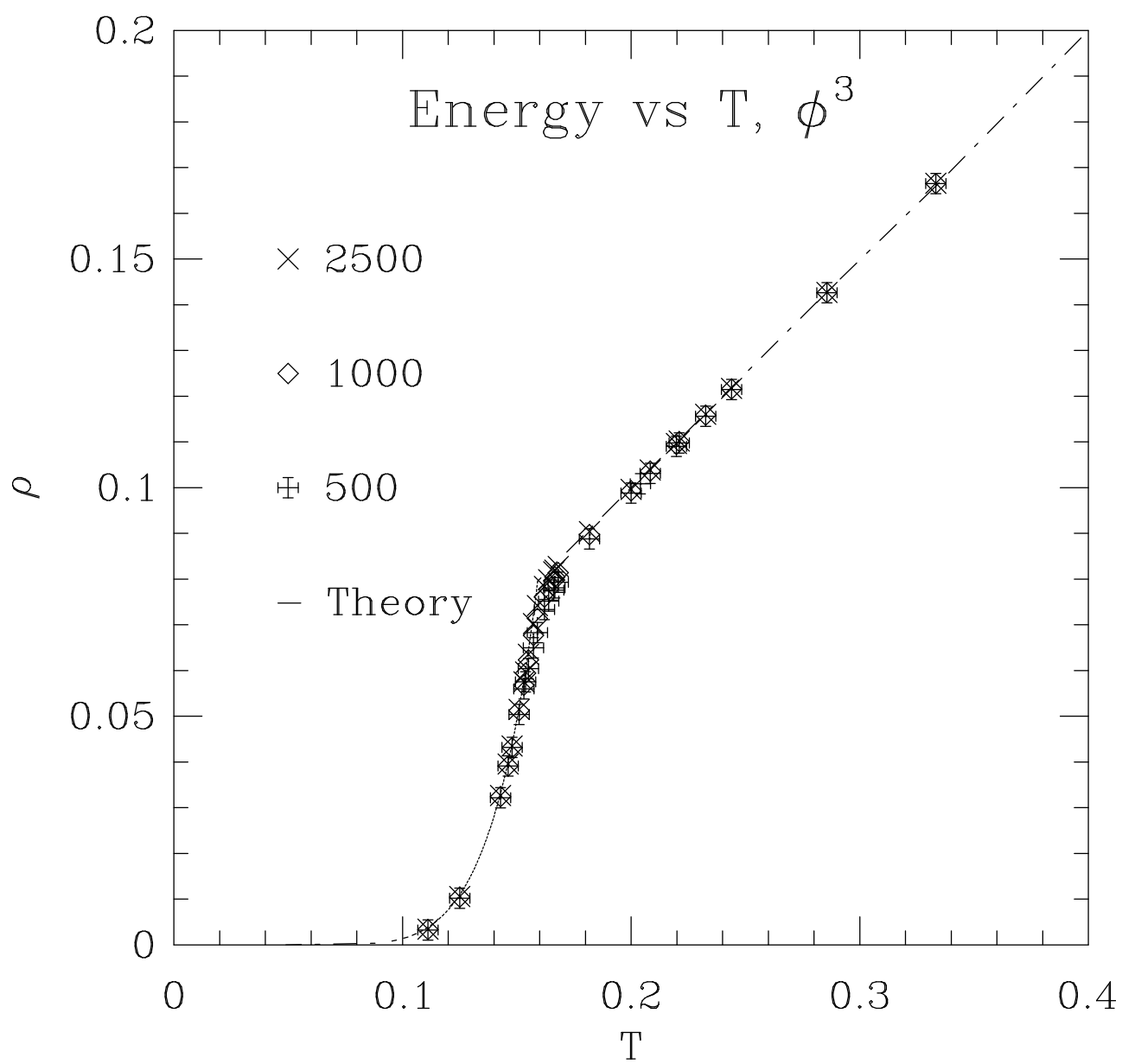
- [1] H.A. Bethe, Proc. Roy. Soc. **A 150** (1935) 552;  
C. Domb, Advan. Phys. **9** (1960) 145;  
T.P. Eggarter, Phys. Rev. **B9** (1974) 2989;  
E. Müller-Hartmann and J. Zittartz, Phys. Rev. Lett. **33** (1974) 893.
- [2] M. Mezard and G. Parisi, Europhys. Lett. **3** (1987) 1067;  
I. Kanter and H. Sompolinsky, Phys. Rev. Lett. **58** (1987) 164;  
K. Wong and D. Sherrington, J. Phys. **A20** (1987) L793;  
K. Wong and D. Sherrington, J. Phys. **A21** (1988) L459;  
C. de Dominicis and Y. Goldschmidt, J. Phys. **A22** (1989) L775;  
C. de Dominicis and Y. Goldschmidt, Phys. Rev. **B41** (1990) 2184;  
P.-Y. Lai and Y. Goldschmidt, J. Phys. **A23** (1990) 399.
- [3] C. Bachas, C. de Calan and P. Petropoulos, J. Phys. **A27** (1994) 6121;  
C. Baillie, D.A. Johnston and J.-P. Kownacki, Nucl. Phys. **B432** (1994) 551;  
C. Baillie, W. Janke, D.A. Johnston and P. Plechac, Nucl. Phys. **B450** (1995) 730.
- [4] C. Bender and T.T. Wu, Phys. Rev. Lett. **37** (1976) 117.
- [5] N. Dorey and P. Kurzepa, Phys. Lett. **B295** (1992) 51.
- [6] J.M. Kosterlitz and D.J. Thouless, J. Phys. **C6** (1973) 1181;  
J.M. Kosterlitz, J. Phys. **C7** (1974) 1046;  
V.L. Berezinski, JETP **34** (1972) 610.
- [7] D. Gross and I. Klebanov, Nucl. Phys. **B344** (1990) 475;  
D. Gross and I. Klebanov, Nucl. Phys. **B354** (1991) 459;  
D.V. Boulatov and V.A. Kazakov, Nucl. Phys. B (Proc. Suppl.) **25A** (1992) 38.
- [8] C.F. Baillie and D.A. Johnston, Phys. Lett. **B291** (1992) 233;  
S.M. Catterall, J.B. Kogut and R.L. Renken, Nucl. Phys. **B408** (1993) 427.
- [9] J. Villain, J. Phys. (France) **36** (1975) 581.
- [10] J. Le Guillou and J. Zinn-Justin (editors), “Large Order Behaviour of Perturbation Theory”, Amsterdam: North Holland (1989).
- [11] W. Janke and K. Nather, Phys. Lett. **A157** (1991) 11;  
W. Janke and K. Nather, Phys. Rev. **B48** (1993) 7419.
- [12] W. Janke and H. Kleinert, Nucl. Phys. **B270** [FS16] (1986) 135.
- [13] W. Janke, Phys. Lett. **A143** (1990) 107.

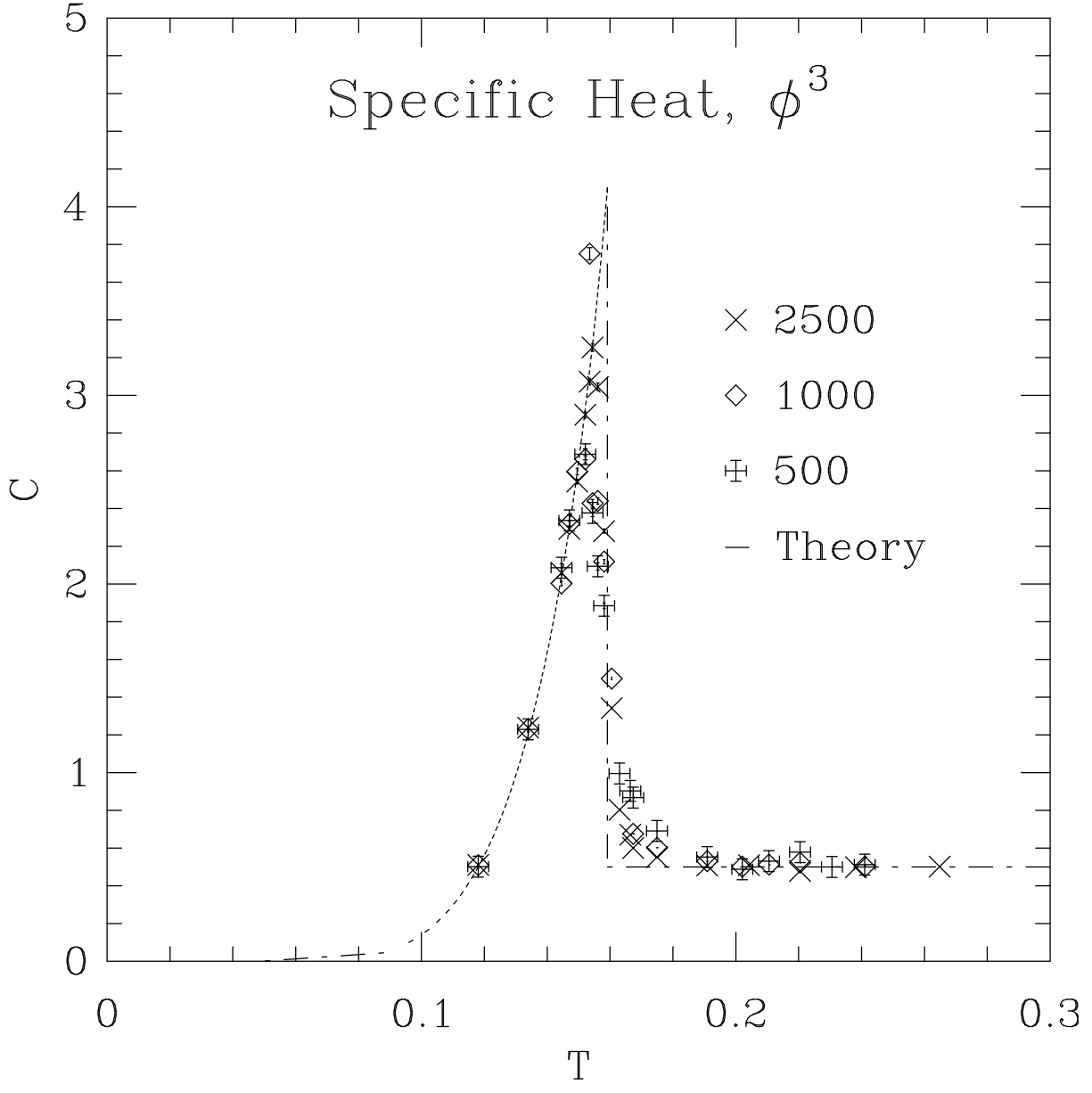
### Figure Captions

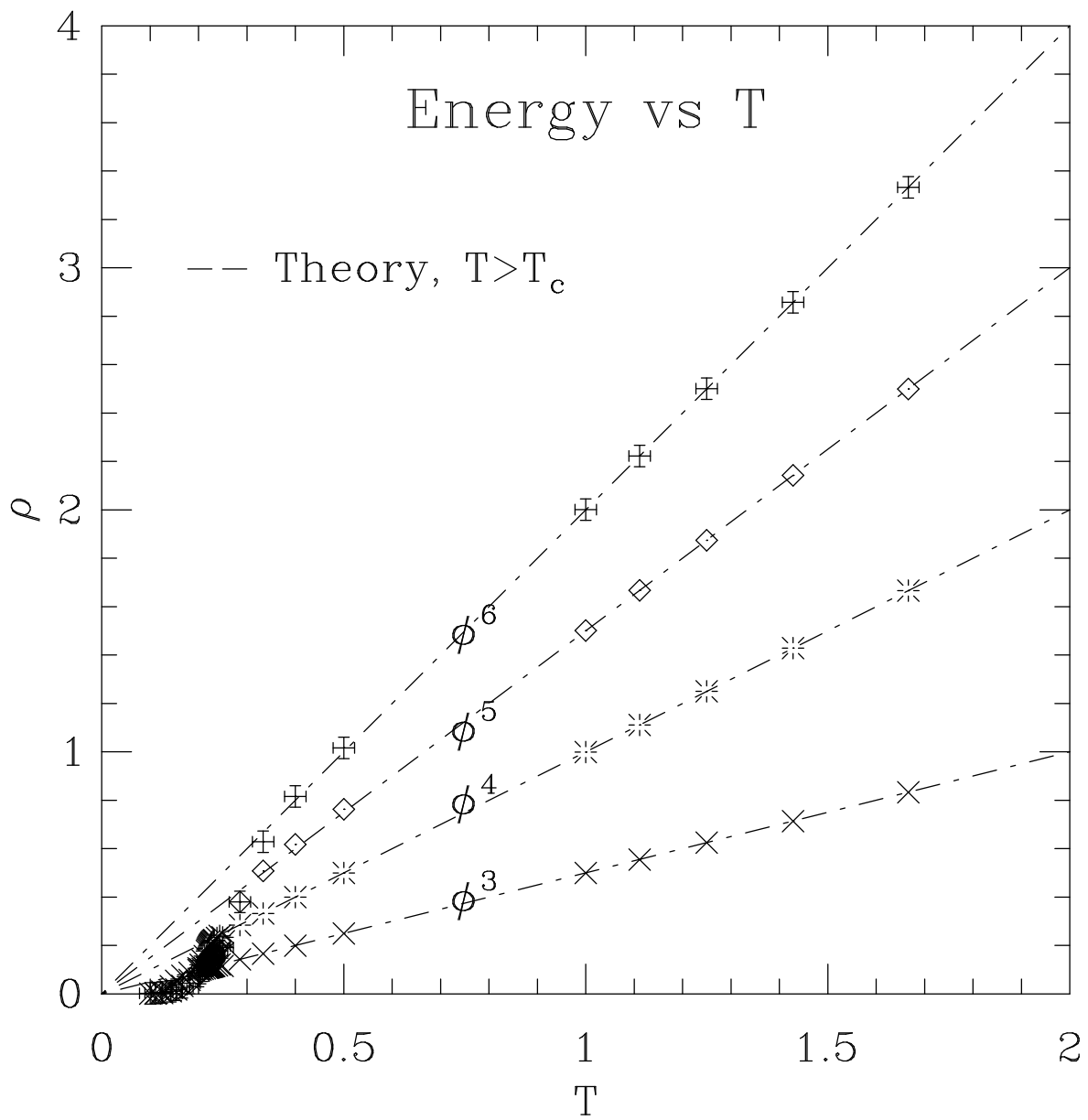
- Fig. 1.** The energy for various  $\phi^4$  graph sizes. A dotted line indicates the analytical prediction.
- Fig. 2.** The specific heat for a  $\phi^4$  graph of size 1000, obtained via both numerical differentiation of  $\rho$  and direct measurement. Again the dotted line represents the analytical curve.
- Fig. 3.** The energy for various  $\phi^3$  graph sizes. The dotted line indicates the analytical prediction.
- Fig. 4.** The specific heat for  $\phi^3$  graphs of various sizes, obtained via numerical differentiation of  $\rho$ . The dotted line shows the analytical prediction.
- Fig. 5.** The energy for  $\phi^3$ ,  $\phi^4$ ,  $\phi^5$  and  $\phi^6$  graphs. The linear prediction,  $\rho = pT$  on  $\phi^{2(p+1)}$  graphs when  $T \geq T_c$ , is shown as dotted lines to emphasize the very good fit.
- Fig. 6.** The specific heat for the *standard* XY model on  $\phi^3$  graphs of various sizes.











# Specific Heat, XY

